Metrol. Meas. Syst., Vol. 31 (2024) No. 1, pp. 23–35
DOI: 10.24425/mms.2024.148534

PAN POLSKA AKADEMIA NAUK

METROLOGY AND MEASUREMENT SYSTEMS
Index 330930, ISSN 0860-8229
www.metrology.wat.edu.pl

M&MS

CALIBRATION OF A BACKGROUND-ORIENTED SCHLIEREN (BOS) IMAGING BASED ON THE LIGHT DEFLECTION ANGLE OF A WEDGE PRISM

Margi Sasono[1)], Setyawan P. Sakti[2)], Johan A. E. Noor[2)], Hariyadi Soetedjo[1)]

1) Study Program of Physics, Ahmad Dahlan University, Yogyakarta, Indonesia (✉ *margi.sasono@fisika.uad.ac.id*)
2) Department of Physics, University of Brawijaya, Malang, East Java, Indonesia

Abstract

The background oriented schlieren (BOS) imaging relies on measuring the light deflection angle in proportion to the refractive index gradient due to the change in the density of a medium. BOS imaging is sensitive to light deflection, and the quantitative measurement requires a reliable calibration method. It is convenient to calibrate the BOS based on the measurement of light deflection. All current BOS calibrations use the random dot as the background and *digital image correlation* (DIC) as the processing algorithm. Such calibrations can induce an inaccurate measurement. This paper proposes a new method to calibrate the BOS based on measuring a known light deflection angle of a wedge prism. The proposed method uses a fringe pattern instead of the random-dot and works based on phase demodulation. The fringe patterns are phase modulated by the wedge prism (the schlieren object). The demodulation utilizes the *Hilbert transform* (HT) on the BOS images, giving the phase difference of the images. The BOS converts the phase difference into the deflection angle. The calibration relies on the deviation of the angle measured by the BOS with the known angle of a wedge prism. The results show that the measurement accuracy of the BOS can achieve more than 95%. This result shows high accuracy in measuring the light deflection angle. Also, the proposed method is more accurate than other methods, and fringe patterns outperform random dot patterns in BOS imaging. Soon, this proposed calibration method can be adopted to validate the instruments for measuring the physical properties of a transparent medium in two-dimensional (2-D) visualization, in a contactless and non-intrusive manner.

Keywords: calibration, background-oriented schlieren (BOS), light deflection angle, wedge prism, standard.

1. Introduction

Background-oriented schlieren (BOS) imaging, as outlined in literature [1, 2], eliminates the need for the equipment of a traditional optical schlieren system. BOS imaging is more straightforward and quantitative than optical interferometry, schlieren, or shadowing techniques. Generally, OS imaging exploits deflection of light by a spatial gradient of the refractive index in an object under test (the schlieren object). The first step is to measure the light deflection angle when the light passes through the schlieren object between the camera (sensor) and the background

Article history: received June 1, 2023; revised August 22, 2023; accepted October 6, 2023; available online December 8, 2023.

patterns. Technically, a digital camera captures the images with and without a schlieren object, giving distortion and reference images, respectively. Comparing both images yields the estimation of the light deflection angle that contains quantitative information about the spatial gradient of the refractive index in the schlieren object.

Recently, BOS imaging has proliferated thanks to the advent of high-resolution digital cameras and improved digital image processing. This fact makes BOS imaging a new and valuable visualization technique. So far, BOS imaging has found many applications to visualize various fluid media, such as fluid flow [3], aerodynamics fields [4], the atmosphere [5, 6], ultrasound field [7], and the shock wave [8]. BOS imaging is not only capable of visualizing qualitative information of the schlieren object (e.g., fluid flow) but also quantitative measurements, such as the refractive index [9, 10] and fluid density [11]. The measurements rely on analysing a distorted image of the background pattern produced by the deflection of the light rays due to the refractive index gradient in the schlieren object. Thus, the design of the background pattern plays an essential role in the better performance of the quantitative measurement. The patterns with high-resolution (high spatial frequency), types of patterns (random dot or periodic), and high-contrast patterns are widely preferred to implement BOS imaging [12]. Generally, a random dot pattern becomes a background pattern in BOS imaging [1, 2]. However, implementing BOS imaging is also recently considering an application with periodic pattern types as the background [13, 14].

Quantitative BOS imaging relies on measuring the refractive index gradient due to the change in density of a medium (the schlieren object). The measured light deflection angle also has a proportion to the refractive index gradient. Thus, BOS imaging is experimentally sensitive to light deflection, and the quantitative evaluation requires a reliable calibration method. Therefore, it is convenient to calibrate BOS imaging based on the measurement of light deflection. So far, there has been limited literature discussing BOS calibration. Porta *et al.* in [15] elaborate on the calibration of BOS using two different gases with known parameters to obtain the density and refractive index. Using the gases as standard materials of BOS calibration could be ineffective. In [4] Ding *et al.* use the plano-convex lens to calibrate BOS technique. In this calibration, the final results are in the form of a qualitative image representing the optical properties of the plano-convex lens. In [16] van Hinserg *et al.* apply a wedge prism as the standard for calibrating the quantitative light deflection angle of BOS imaging. However, all literature uses the random dot as the background and the digital image correlation (DIC) as the image processing algorithm without including uncertainty evaluation. Using a random dot in BOS imaging introduces an inhomogeneous distribution in the background plane [13, 14], and the dot can experience a shape distortion due to large density gradients [17]. In addition, the DIC algorithm also has drawbacks, for example, assuming that the displacement image is approximately constant. Thus, violating this condition could introduce significant uncertainty in measurement [13]. Therefore, calibrations using these techniques can induce an inaccurate measurement result.

This paper proposes a new method to calibrate BOS imaging. The calibration process relies on measuring a known light deflection angle of a wedge prism, similar to that in [16]. However, the proposed method uses a periodic fringe pattern instead of a random-dot background. The spatial frequency of a fringe pattern background acts as a carrier frequency that is phase modulated by the schlieren object, giving a phase modulation image. This work demodulates the phase modulation image, similarly to the method used in the communication field [18]. Research has shown that the phase demodulation method offers an accurate result, for example, in designing phase microscopy [19]. This work proposes a method for phase demodulation using the *Hilbert transform* (HT) of both images, either the distortion (modulated image) or the reference (carrier frequency) image. Finally, the calibration process converts the extracted (demodulated) phase to the light deflection angle.

Metrol. Meas. Syst., Vol. 31 (2024), No. 1, pp. 23–35
DOI: 10.24425/mms.2024.148534

The calibration procedure assumes a known light deflection angle of a wedge prism (as stated in the manufacturer manual) as a measurement target (standard angle). Otherwise, the light deflection angle measured by BOS imaging is the measured angle. The calibration process tests the measurement accuracy and uncertainty evaluation level by assessing the differences between the standard and measured angle. Using a wedge prism to calibrate BOS imaging will ensure accuracy and efficiency in the measurement of the deflection angle. Accurate measurement of the light deflection angle is the entry point for quantitative measurements, such as the refractive index of the medium, the density of the fluids, the temperature of the gases, and other physical properties of transparent mediums. Soon, the proposed calibration method can be adopted to validate BOS imaging instruments for measuring quantitative physical properties, such as refractive index, density, and temperature of the transparent medium in 2-D visualization in a contactless and non-intrusive manner.

2. Method

2.1. BOS principle based on phase demodulation

The propagation of light rays in the refractive index gradient (the schlieren object) is subject to deflection. The magnitude of deflection depends on the change in the refractive index inside the density gradients of a schlieren object. Generally, Fermat's principle reveals that the propagation of a light ray through a schlieren object (inhomogeneous medium) as [20]

$$\frac{\mathrm{d}}{\mathrm{d}s}\left(n\frac{\mathrm{d}\vec{r}}{\mathrm{d}s}\right) = \nabla n, \tag{1}$$

where $\mathrm{d}s$ is the trajectory element of the ray path length, $\mathrm{d}\vec{r}$ is the element of a ray position vector, n is the refractive index as a function of position, and ∇n is the refractive index gradient in the Cartesian Coordinate System. Figure 1 shows the propagation of a light ray along the Z-axis. Thus, the trajectory element of the path length can be changed into $\mathrm{d}s = \mathrm{d}z$, and there is no gradient of the refractive index along the Z-axis. Practically, the gradient of refractive index only occurs along the X-axis and Y-axis.

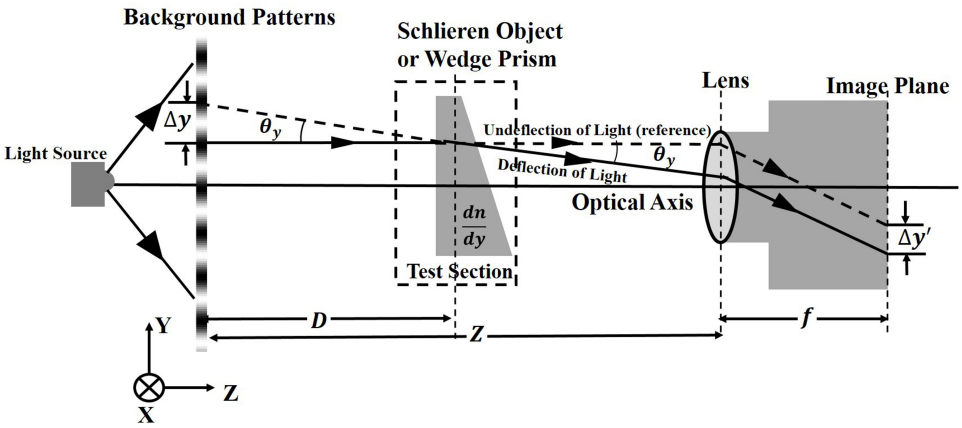

Fig. 1. Schematic diagram of a BOS imaging setup using a wedge prism as the schlieren object.

The basic concept of the BOS system is simple, as shown in Fig. 1. By assuming that the light rays propagate paraxially in the Z-axis direction and the deflection angle is very small, (1) could be decomposed to the Y-axis as [21]

$$\frac{\mathrm{d}^2 y}{\mathrm{d}z^2} = \frac{1}{n}\left(\frac{\mathrm{d}n}{\mathrm{d}y}\right). \tag{2}$$

Thus, by integrating (2) once to z, the deflection angle θ_y (as shown in Fig. 1) can be determined as

$$\theta_y \approx \left(\frac{\mathrm{d}y}{\mathrm{d}z}\right) = \left(\frac{\Delta y}{D}\right) = \frac{1}{n_0}\int\left(\frac{\mathrm{d}n}{\mathrm{d}y}\right)\mathrm{d}z, \tag{3}$$

where n_0 is the reference of the refractive index and n is the refractive index of the schlieren object under test. Referring to Fig. 1, D is the schlieren object-to-background distance and Δy corresponds to the displacement of the background patterns (distorted image) due to the gradient of the refractive index in the Y-axis direction $\left(\frac{\mathrm{d}n}{\mathrm{d}y}\right)$.

Figure 2 illustrates the BOS imaging principle based on phase demodulation. As the background is a fringe pattern, it is also called the spatial carrier frequency. For simplicity, there is no spatial carrier frequency on the X-axis (the fringe pattern along the X-axis). When BOS imaging, as shown in Fig. 1, is without a schlieren object (no refractive index gradient), the spatial carrier frequency is a reference fringe pattern (reference image). Mathematically, a sinusoidal intensity of the reference image along the Y-axis, $I_\mathrm{o}(y)$, can be represented as

$$I_\mathrm{o}(y) = I_\mathrm{o}\cos(2\pi\upsilon_y + \varphi_\mathrm{o}), \tag{4}$$

where I_o is maximum intensity, υ_y is the spatial fringe frequency in the Y-axis, and φ_o is the initial phase (phase offset). As in (4), intensity cannot carry the desired schlieren object information. Therefore, (4) needs to be modulated by a schlieren object. The schlieren object will introduce

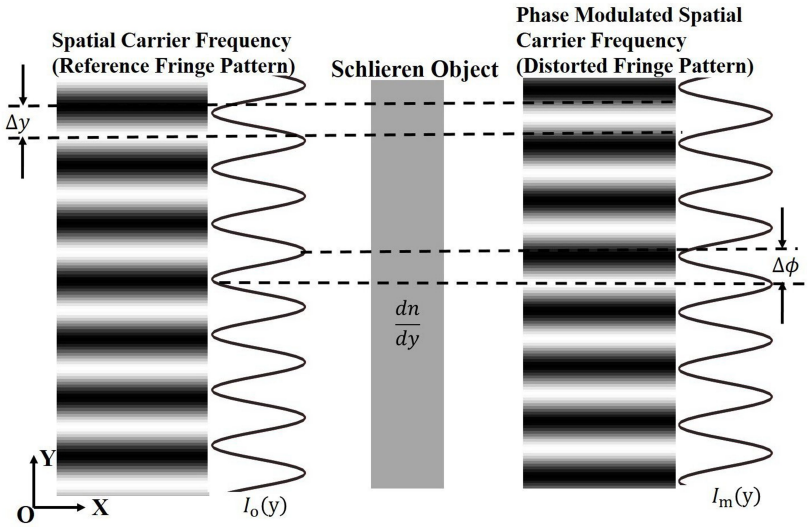

Fig. 2. Illustration of the fringe patterns displacement and phase difference caused by the schlieren object.

a displacement of fringe patterns. This condition allows a phase-modulated spatial fringe frequency or a distorted (phase modulation) image. Mathematically, the modulation intensity, $I_m(y)$, can be revealed as

$$I_m(y) = I_o \cos(2\pi \upsilon_y + \varphi_m), \tag{5}$$

where φ_m is phase-modulation of spatial carrier frequency caused by the schlieren object. The subtraction of (6) from (5) gives the phase difference $\Delta\phi$ (in rad) in proportion to the displacement fringe patterns Δy as

$$\Delta\phi = \varphi_m - \varphi_o = 2\pi \upsilon_y(\Delta y). \tag{6}$$

So, the main problem is to estimate the phase difference $\Delta\phi$ of (6) to obtain the displacement fringe patterns Δy. Finally, the estimated displacement fringe patterns convert into the light deflection angle $\theta_{\mathbf{y}}$ as in (3), proportional to the gradient of refractive index $\left(\frac{\mathrm{d}n}{\mathrm{d}y}\right)$.

2.2. Phase Demodulation (Phase extraction)

The phase difference in (6) is crucial in estimating the physical quantities of the schlieren object (in this case, the light deflection angle of a wedge prism). This work uses the *Hilbert transform* (HT) [21, 23] to demodulate the phase-modulation of (5). The intensity of (4) and (5) are the real-value data or data from the experiment [21]. According to the signal theory, the HT of (4) and (5) generally gives a complex-valued signal called the analytic signal, $Z(y)$ as [22]

$$Z(y) = X_R(y) + iX_{IM}(y) = A(y)e^{i\phi(y)}, \tag{7}$$

where $X_R(y)$ is the real-value data (signal), $i = \sqrt{-1}$ is the imaginary number, $X_{IM}(y)$ is imaginary-value data, $A(y)$ is amplitude modulation (the envelope of the signal), and $\phi(y)$ represents the phase of the signal. Here, the $X_{IM}(y)$ is the HT of the $X_R(y)$. Based on (7), it is convenient to obtain the extracted phase $\phi(y)$ as

$$\phi(y) = \arctan\left[\frac{X_{IM}(y)}{X_R(y)}\right] \quad \text{(in rad)}. \tag{8}$$

Mathematically, the extracted phase $\phi(y)$ in (8) is the wrapped phase in the range $(-\pi, +\pi)$. Therefore, the phase in (8) needs an unwrapping process to extract the absolute (actual) phase. The literature [23, 24] elucidates in detail the algorithm for the unwrapping process.

Figure 3 shows a flowchart of the phase extraction process based on demodulation HT in BOS imaging. Firstly, a camera captures and records the images (reference and distorted images). Applying HT in the column-by-column manner of the image pixels converts the real-value images into complex-valued images, containing real and imaginary parts. The phase of the complex-valued images can be extracted by (8). The phase resulting from this step is the wrapped phase in the range $(-\pi, +\pi)$. The following step is the unwrapping process to convert the wrapped-phase into the unwrapped-phase images (desired phase). And then, subtracting both the unwrapped-phase images gives the desired phase-difference containing the quantitative physical of the schlieren object (in this case, optical characteristics of the wedge prism). The next step converts the phase difference into the displacement of fringe patterns using (6). Finally, the process quantifies (converting) the displacement of fringe patterns into the light deflection angle using (3).

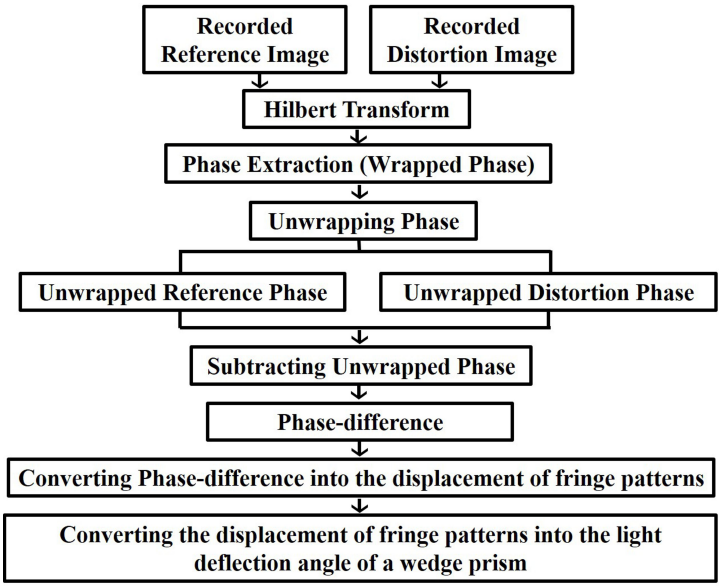

Fig. 3. Flowchart of the phase extraction process based on demodulation HT in the BOS experiment.

2.3. Experimental Setup

The BOS imaging setup is simple as it requires only two principal components (background patterns and a single camera). The simplicity of the setup significantly reduces the complexity associated with aligning the optical components [1]. Figure 4 shows a photograph of the developed BOS imaging setup. A light source is a white light emitting diode (LED) panel to illuminate the fringe patterns background printed on transparent materials for (30 × 30) cm. The colour combination of fringes is black-white to provide a highly contrasting background. The printed fringe thickness is d_{frg} = 1 mm. As captured by the camera, the background design has an intensity profile of sinusoidal patterns with a spatial carrier frequency, υ_y = 0.04 cycle/pixel or spatial carrier period, p_y = 25 pixels along the Y-axis. This work used a Hayear CCD digital camera to provide an image resolution of (1800 × 1920) pixels and the spatial resolution of 1.43 μm/pixel. The lens attached to the camera was a Fujian lens with a focal length f = 50 mm. Also, the camera had a connection system to a personal computer (PC) for recording the images. During the experiments, the camera lens focuses on the background patterns. Literature [4] explains the sensitivity and resolution during the BOS image recording process. As shown in Fig. 4, the background patterns are adjusted at a distance Z = 1500 mm from the lens. Thus, the background has a position at infinity ($Z \gg f$), and light rays emanating from the background patterns are assumed to be parallel (or using the paraxial approximation). The setup using the paraxial approximation can ignore errors caused by the alignment of optical components, as described in the literature [9].

In this experiment, the schlieren object is a wedge prism of 4 × 4 cm in size with a known light deflection angle of 0.57° according to the manufacturer's manual sheets). As shown in Fig. 4, the position of the wedge prism is at a distance of D = 500 mm from the background. Optically, a wedge prism has uniform (constant) refractive index gradients [19]. Thus, the light ray passing through the wedge prism will deflect at the single light angle. This angle is a standard (target)

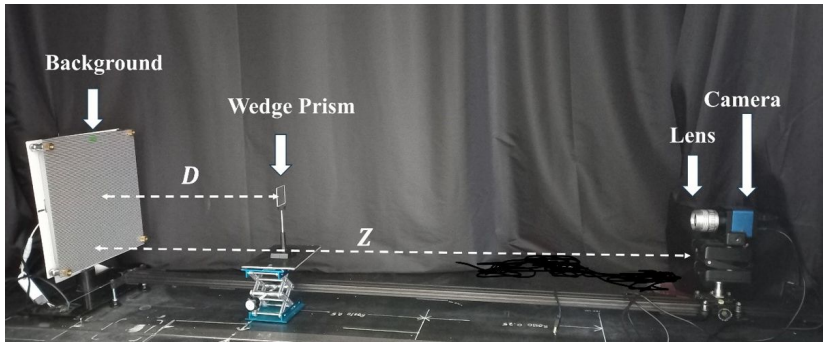

Fig. 4. Photograph of the BOS imaging setup.

measured by BOS imaging in the calibration principle. As expected, the deflection angle of light rays will distort the background patterns and introduce uniform fringe pattern displacements. BOS imaging can convert the displacements into light deflection angles. The uniformity of angles represents the refractive index or density gradient at each point (or distribution) in the wedge prism area. The calibration assesses the difference between the standard and angle measured by the BOS technique to determine the measurement accuracy level.

3. Results and discussion

In this work, the digital camera captures the fringe patterns background in the grey-level images in proportion to the light intensity detected by the camera sensor. Firstly, the digital camera captures the reference image without a wedge prism in the test section of the BOS imaging setup (as shown in Fig. 4). The photograph in Fig. 5a shows raw data (grey-level) of a reference image. Next, the placement of a wedge prism in the test section displaces the background fringes pattern giving a distorted image as shown in a photograph in Fig. 5b. In other words, the image of the spatial carrier frequency experiences phase modulation caused by the presence of a wedge prism. Visually, as shown in Fig. 5b, the fringe displacements appear in a single direction (Y-axis), indicating uniformity. Optically, the gradient of the refractive index in the area of the wedge prism (indicated by arrows) introduces a single light deflection inducing a distorted image as captured by the camera. The comparison of the intensity profiles along the white dashed line in both images clearly shows the phase difference, as shown in Fig. 5c. Hence this work uses the phase demodulation HT to extract and convert the phase difference into the light deflection angle of a wedge prism.

The phase demodulation HT initially transforms the data in both images (reference and distorted images) in a column-by-column manner. The transformation results are the complex-valued images. The next step extracts the phase images by using (8), as shown in Fig. 6a (reference) and Fig. 6b (distortion). However, the images (as in Figs. 6a and 6b) are mathematically wrapped phases in the range $(-\pi, +\pi)$. The unwrapping process yields the continuous phase images, as shown in Figs. 6c and 6d. These images describe the desired (actual) phase. As can be seen in Figs. 7a and 7b, the plot of phase profiles in the images (along the white dashed line) support the results. The profile of wrapped phase images shows the curves limited in the range $(-\pi, +\pi)$ or the discontinuous valued phase. In comparison, the profile of unwrapped phase images shows the continuity or linearity in the Y-axis (in pixel units) according to the physical characteristics of phase in (4) or (5).

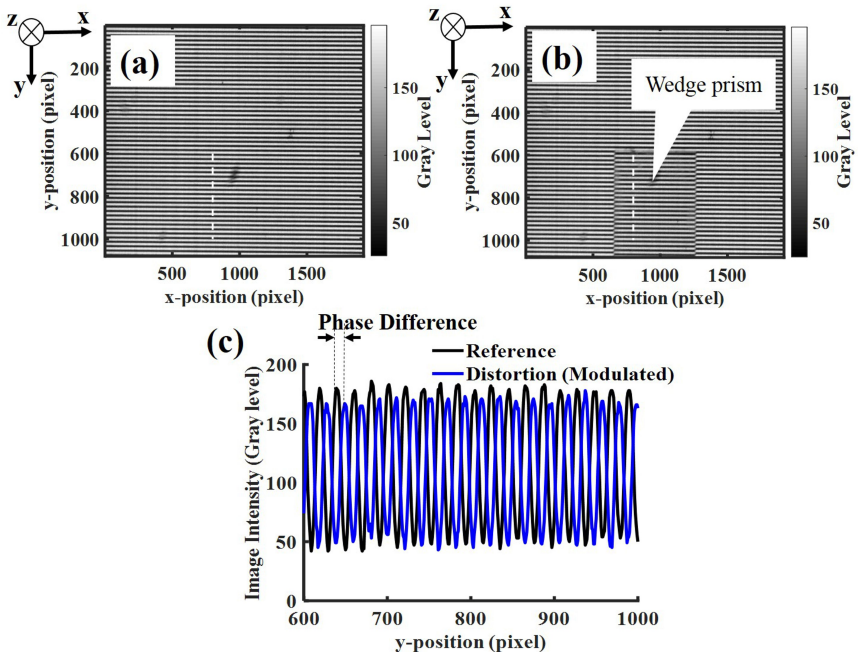

Fig. 5. (a) Photograph of the reference raw image, (b) photograph of the distorted (phase-modulated) raw image aa caused by the presence of a wedge prism, (c) comparison of the intensity profiles along the white dashed line in both photographs (images).

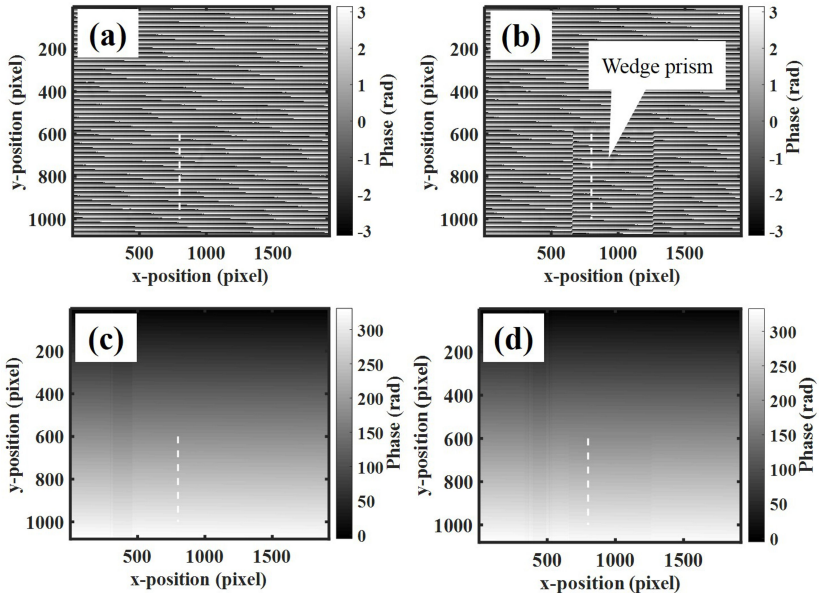

Fig. 6. (a) wrapped phase image of reference, (b) wrapped phase image of distortion (with a wedge prism), (c) unwrapped phase image of reference, (d) unwrapped phase image of distortion.

Metrol. Meas. Syst., Vol. 31 (2024), No. 1, pp. 23–35
DOI: 10.24425/mms.2024.148534

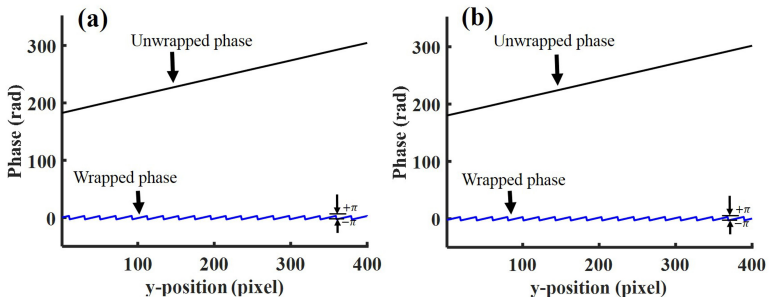

Fig. 7. Plot of phase profiles in the images (along the white dashed line) of Fig. 6. (a) Wrapped and unwrapped phase of reference, (b) wrapped and unwrapped phase of distortion.

Subtraction of the unwrapped phase image in Fig. 6d (distorted) from Fig. 6c (reference) yields a phase difference image. This image contains quantitative information on the optical characteristics of a wedge prism (the schlieren object). As in (6), the phase difference data is proportional to the fringe pattern displacements. Finally, BOS imaging converts the phase differences data into the data of the light deflection angles of the wedge prism using (3). The images in Figs. 8a and 8b represent the data distribution of phase difference and the light deflection angles measured by BOS imaging. Visually, both images show a similarity and high homogeneity, reflecting the optical characteristics of the wedge prism. The graphics in Figs. 8c and 8d show the profiles along the vertical and horizontal white dashed line across the image plane of the light deflection angles (Fig. 8b), respectively. The graphic curves show that all measured data approach the standard line angle of 0.57° as indicated by the blue dashed line. Qualitatively, the results show that BOS imaging accurately measures the wedge prism with a known light deflection angle of 0.57°.

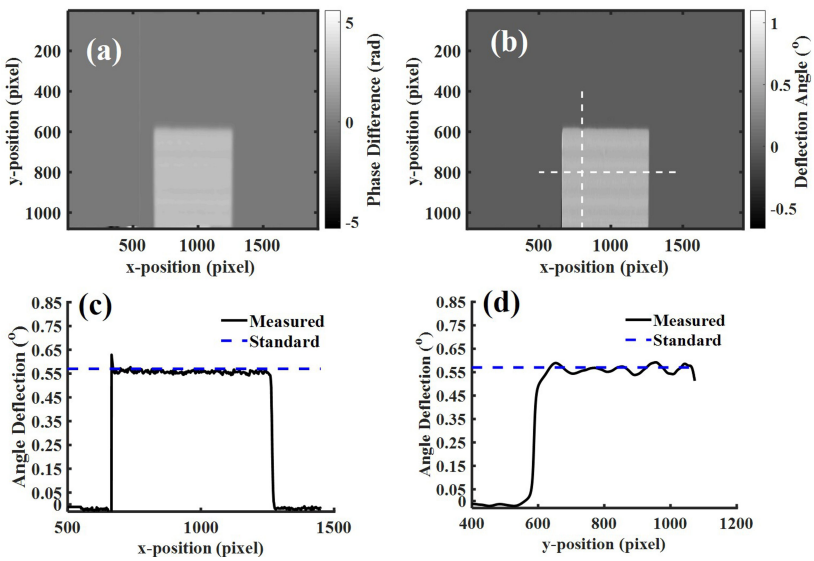

Fig. 8. (a) Image of phase-difference, (b) image of deflection angle, (c) horizontal and (d) vertical plot of the deflection angle profile along the white dashed line in the image (b).

The assessment of measurement accuracy relies on the subtraction of the measured angle data from standard angle data (an angle of 0.57°), which will produce the measurement error. The plotted data (only 20 data) with the error bars in Fig. 9a shows a result of the measured light deflection angles along the vertical profile (Fig. 8c). The measured data spatially fluctuate around the standard line. The small error bars on each data point indicate a closeness of measurement results with the standard angle of 0.57°. On the other hand, Fig. 9b shows that the error bars of the measurements in the horizontal profile (Fig. 8d) appear more significant than the vertical profile (Fig. 8c). The HT process in the vertical direction (column-by-column) in the images might cause the measurement results with great error bars.

In this work, the statement of measurement accuracy uses the percentage of error and the best measurement result (average of measurement data) with uncertainty. As seen in Figs. 9c and 9d, all measurement generally gives an error percentage of ±1% to ±2% (less than 3%). The results show that the measurement accuracy of BOS imaging can reach more than 97%. The results of BOS imaging measuring the light deflection angle of a wedge prism are (0.561 ± 0.013)° in the vertical direction, and (0.556 ± 0.013)° in the horizontal direction. Generally, all data of the light deflection angles show a uniformity near the standard angle of 0.57° across the area of the wedge prism. Also, the results describe the real optical characteristics of a wedge prism. Therefore, the developed BOS imaging is highly accurate in the light deflection angle measurement.

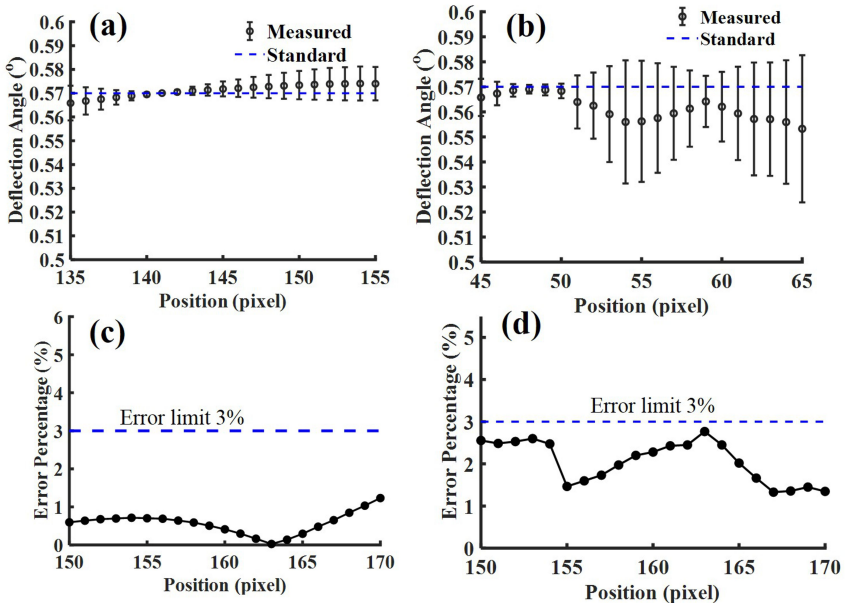

Fig. 9. Plotted measurement data with error bars (a) horizontal and (b) vertical profile of deflection angle image. Error percentage (less than 3%) of (c) vertical and (d) horizontal profile of the deflection angle image.

Also, this work attempts to compare the performance of the proposed method with the existing literature in calibrating BOS imaging. Although based on different BOS imaging setups, Table 1 gives a comparison of the calibration results. The performance comparison relies on quantitative error percentage assessment. As shown in the table, the proposed method provides calibration results with the smallest error percentage compared to the others. Despite using two wedge prisms with different light deflection angles as calibration standards, the proposed method also appears to

have a smaller error percentage when compared to the literature [16]. From Table 1, the proposed method is more accurate than other calibration methods. It can also be concluded that periodic patterns (fringe patterns) outperform random dot patterns as the background in BOS imaging.

Table 1. Comparison of the calibration results.

Literatures/ Proposed Method	**Type of background pattern**	**Image Processing Method**	**Standard (schlieren object for calibration)**	**Result in error percentage (%)**	**Type of measurements**
[4]	Random dot	DIC	Plano-Convex Lens	–	Qualitative
[15]	Random dot	DIC	Gases	6.9	Quantitative
[16]	Random dot	DIC	Wedge Prism (light deflection angle of 1°)	3	Quantitative
Proposed Method	Fringe Pattern	Phase	Wedge Prism (light deflection angle of 0.57°)	1–2	Quantitative

4. Conclusions

The fringe patterns as the background and a wedge prism as a schlieren object have successfully calibrated the BOS imaging based on the measurement of the light deflection angle. The measurement relies on the phase demodulation HT of displaced fringe patterns (distorted image) due to the wedge prism in the test section of the BOS imaging setup. The demodulation process obtains a phase difference between the reference and distortion images captured by a digital camera. BOS imaging converts and reconstructs the phase difference into the image of the light deflection angles. The calibration procedure assesses the measurement accuracy through the deviation of the angle measured with BOS imaging with the known angle of 0.57° introduced by a wedge prism. The calibration results show that the measurement accuracy of the developed BOS imaging can reach more than 97%. The results of BOS imaging measured across the image of light deflection angle are $(0.561 \pm 0.013)^\circ$ in the vertical direction and $(0.556 \pm 0.013)^\circ$ in the horizontal direction. Generally, the results show a uniformity near the standard angle across the image area and describe the optical characteristics of a wedge prism. Also, the results of a comparison show that the proposed method is more accurate than other calibration methods and fringe patterns outperform random dot patterns as the background in BOS imaging. Thus, using a wedge prism in the calibration of BOS imaging ensures the high accuracy level of light deflection angle measurement simply and easily. Soon, the proposed calibration method can be adopted to validate a BOS imaging instrument for measuring quantitative the physical properties such as refractive index, density, and temperature of a transparent medium in 2-D visualization in a non-contact and non-intrusive manner.

Acknowledgements

We would like to thank the Management of Metrology Laboratory at Ahmad Dahlan University for financial and facility support. Special thanks to Mr. Apik Rusdiarna IP of the Study Program of Physics (Metrology-Electronic Materials-Instrumentation), Faculty of Applied Science and Technology, Ahmad Dahlan University, Yogyakarta, Indonesia for his sharing of knowledge and discussion on MATLAB programs and the use a CCD camera.

References

[1] Raffel, M. (2015). Background-oriented schlieren (BOS) techniques. *Experiments in Fluids*, *56*(3), 1–17. https://doi.org/10.1007/s00348-015-1927-5

[2] Kaganovich, D., Johnson, L. A., Mamonau, A. A., & Hafizi, B. (2020). Benchmarking background oriented schlieren against interferometric measurement using open source tools. *Applied Optics*, *59*(30), 9553. https://doi.org/10.1364/ao.406301

[3] Becher, L., Voelker, C., Rodehorst, V., & Kuhne, M. (2020). Background-oriented schlieren technique for two-dimensional visualization of convective indoor air flows. *Optics and Lasers in Engineering*, *134*(April), 106282. https://doi.org/10.1016/j.optlaseng.2020.106282

[4] Ding, H., Yi, S., & Zhao, X. (2019). Experimental investigation of aero-optics induced by supersonic film based on near-field background-oriented schlieren. *Applied Optics*, *58*(11), 2948. https://doi.org/10.1364/ao.58.002948

[5] Barinov, Y. A. (2021). Features of the background oriented schlieren method for studying small axisymmetric plasma objects. *Journal of Visualization*, *24*(6), 1131–1139. https://doi.org/10.1007/s12650-021-00763-1

[6] Heineck, J. T., Banks, D. W., Smith, N. T., Schairer, E. T., Bean, P. S., & Robillos, T. (2021). Background-oriented schlieren imaging of supersonic aircraft in flight. *AIAA Journal*, *59*(1), 11–21. https://doi.org/10.2514/1.J059495

[7] Luo, H., Kusunose, J., Pinton, G., Caskey, C. F., & Grissom, W. A. (2020). Rapid quantitative imaging of high intensity ultrasonic pressure fields. *The Journal of the Acoustical Society of America*, *148*(2), 660–677. https://doi.org/10.1121/10.0001689

[8] Ichihara, S., Shimazaki, T., & Tagawa, Y. (2022). Background-oriented schlieren technique with vector tomography for measurement of axisymmetric pressure fields of laser-induced underwater shock waves. *Experiments in Fluids*, *63*(11), 1–18. https://doi.org/10.1007/s00348-022-03524-4

[9] Beermann, R., Quentin, L., Pösch, A., Reithmeier, E., & Kästner, M. (2017). Background oriented schlieren measurement of the refractive index field of air induced by a hot, cylindrical measurement object. *Applied Optics*, *56*(14), 4168. https://doi.org/10.1364/ao.56.004168

[10] Grauer, S. J., & Steinberg, A. M. (2020). Fast and robust volumetric refractive index measurement by unified background-oriented schlieren tomography. *Experiments in Fluids*, *61*(3), 1–17. https://doi.org/10.1007/s00348-020-2912-1

[11] Kaneko, Y., Nishida, H., & Tagawa, Y. (2021). Background-oriented schlieren measurement of near-surface density field in surface dielectric-barrier-discharge. *Measurement Science and Technology*, *32*(12). https://doi.org/10.1088/1361-6501/ac1ccc

[12] Shimazaki, T., Ichihara, S., & Tagawa, Y. (2022). Background oriented schlieren technique with fast Fourier demodulation for measuring large density-gradient fields of fluids. *Experimental Thermal and Fluid Science*, *134*, 110598. https://doi.org/10.1016/j.expthermflusci.2022.110598

[13] Wildeman, S. (2018). Real-time quantitative Schlieren imaging by fast Fourier demodulation of a checkered backdrop. *Experiments in Fluids*, *59*(6). https://doi.org/10.1007/s00348-018-2553-9

[14] Psota, P., Stašík, M., Kredba, J., Lédl, V., Jašíková, D., Kotek, M., & Kopecký, V. (2022). Quantitative Schlieren imaging based on fringe projection. *EPJ Web of Conferences*, *264*, 01034. https://doi.org/10.1051/epjconf/202226401034

[15] Porta, D., Echeverría, C., Aguayo, A., Cardoso, J. E. H., & Stern, C. (2016). Recent Advances in Fluid Dynamics with Environmental Applications. *Recent Advances in Fluid Dynamics with Environmental Applications*, 115–124. https://doi.org/10.1007/978-3-319-27965-7

[16] van Hinsberg, N. P., & Rösgen, T. (2014). Density measurements using near-field background-oriented Schlieren. *Experiments in Fluids*, *55*(4), 1–11. https://doi.org/10.1007/s00348-014-1720-x

[17] Meinecke, M., Kilzer, A., & Weidner, E. (2020). Background Orientated Schlieren Method Applied for Liquid Systems of Strong Refractive Gradients. *Chemie-Ingenieur-Technik*, *92*(7), 1089–1097. https://doi.org/10.1002/cite.201900189

[18] Sharma, S., & Kulkarni, R. (2021). Phase demodulation from a spatial carrier fringe pattern using extended complex Kalman filter. *Optics and Lasers in Engineering*, *138* (August 2020), 106409. https://doi.org/10.1016/j.optlaseng.2020.106409

[19] Cai, H., Wang, Y. L., Wainner, R. T., Iftimia, N. V., Gabel, C. V., & Chung, S. H. (2019). Wedge prism approach for simultaneous multichannel microscopy. *Scientific Reports*, *9*(1), 1–10. https://doi.org/10.1038/s41598-019-53581-9

[20] Lin, D., Teichman, J., & Leger, J. R. (2015). Deflectometry for measuring inhomogeneous refractive index fields in two-dimensional gradient-index elements. *Journal of the Optical Society of America A*, *32*(5), 991. https://doi.org/10.1007/s00348-015-1927-5

[21] Yang, Y. (2017). A Signal Theoretic Approach for Envelope Analysis of Real-Valued Signals. *IEEE Access*, *5*(March), 5623–5630. https://doi.org/10.1109/ACCESS.2017.2688467

[22] Yang, Y., & Li, C. (2020). Modulated signal detection method for fault diagnosis. *IET Science, Measurement and Technology*, *14*(10), 962–971. https://doi.org/10.1049/iet-smt.2020.0127

[23] Wynne, L. C., Ballantyne, H. T., Li, X., Di Falco, A., & Schulz, S. A. (2020). A Hilbert transform method for measuring linear and nonlinear phase shifts imparted by metasurfaces. *Photonics and Nanostructures – Fundamentals and Applications*, *42*, 100844. https://doi.org/10.1016/j.photonics.2020.100844

[24] Wu, Z., Guo, W., Lu, L., & Zhang, Q. (2021). Generalized phase unwrapping method that avoids jump errors for fringe projection profilometry. *Optics Express*, *29*(17), 27181. https://doi.org/10.1364/oe.436116

Margi Sasono received the M.Sc. degree from the Department of Physics of Gadjah Mada University (UGM), Yogyakarta, Indonesia in 2004. From 2012 he has been head of the Calibration and Testing Laboratory at Ahmad Dahlan University (UAD) Yogyakarta. He is currently pursuing the Ph.D. degree with the Instrumentation Group, Department of Physics, University of Brawijaya (UB), Malang, East Java, Indonesia.

Johan A.E. Noor is a senior lecturer at the Department of Physics, University of Brawijaya, Malang, Indonesia. He received his Ph.D. degree in biomedical physics from the University of New South Wales, Australia. His research interests include the physics of radiotherapy, radiation protection, naturally occurring radioactive materials (NORMs), toxicity of PM2,5, and electrical impedance of living organisms.

Setyawan Purnomo Sakti received the B.Sc. degree in physics from Gadjah Mada University, Indonesia, in 1989. He obtained his M.Sc. Eng. degree in electrical and electronics engineering from the University of South Australia in 1994. In 2000, he received his Dr.-Ing. degree from the Otto von Guericke Universität, Magdeburg, Germany. Currently, he is a professor at the Department of Physics and head of the Sensor Technology Laboratory, University of Brawijaya. His research interests include sensors, functional materials, Internet of Things, medical technology, rapid detection, and embedded systems.

Hariyadi Soetedjo received his Ph.D. degree in physics from the University of Essex, Colchester, England in 1999. He has been a professor at the Department of Physics, Ahmad Dahlan University, Indonesia since 2014. His main interest is optical physics in material characterizations and applications. He spent many years working as a Visiting Scientist in the USA, Germany, Finland, Sweden, Spain and numerous other countries, researching material characterization based on polarized optics.